



HAL
open science

Asphaltene Cross-flow Membrane Ultrafiltration on a Preparative Scale and Feedstock Reconstitution Method

J. Marques, D. Guillaume, I. Merdrignac, D. Espinat, L. Barré, S. Brunet

► **To cite this version:**

J. Marques, D. Guillaume, I. Merdrignac, D. Espinat, L. Barré, et al.. Asphaltene Cross-flow Membrane Ultrafiltration on a Preparative Scale and Feedstock Reconstitution Method. Oil & Gas Science and Technology - Revue d'IFP Energies nouvelles, 2009, 64 (6), pp.795-806. 10.2516/ogst/2009053 . hal-02001587

HAL Id: hal-02001587

<https://ifp.hal.science/hal-02001587>

Submitted on 31 Jan 2019

HAL is a multi-disciplinary open access archive for the deposit and dissemination of scientific research documents, whether they are published or not. The documents may come from teaching and research institutions in France or abroad, or from public or private research centers.

L'archive ouverte pluridisciplinaire **HAL**, est destinée au dépôt et à la diffusion de documents scientifiques de niveau recherche, publiés ou non, émanant des établissements d'enseignement et de recherche français ou étrangers, des laboratoires publics ou privés.

Asphaltene Cross-flow Membrane Ultrafiltration on a Preparative Scale and Feedstock Reconstitution Method

J. Marques^{1*}, D. Guillaume¹, I. Merdrignac¹, D. Espinat¹, L. Barré² and S. Brunet³

¹ Institut français du pétrole, IFP-Lyon, Rond-point de l'échangeur de Solaize, BP 3, 69360 Solaize - France

² Institut français du pétrole, IFP, 1-4 avenue de Bois-Préau, 92852 Rueil-Malmaison - France

³ Laboratoire de chimie, 7B Catalyse en Chimie Organique, UMR 6503, Faculté des Sciences de l'Université de Poitiers, 86022 Poitiers Cedex - France

e-mail: joao.marques@ifp.fr - denisjm.guillaume@ifp.fr - isabelle.merdrignac@ifp.fr - didier.espinat@ifp.fr
loic.barre@ifp.fr - sylvette.brunet@univ-poitiers.fr

* Corresponding author

Résumé — Ultrafiltration des asphaltènes par filtration tangentielle et méthodologie de reconstitution des charges — Afin de mieux comprendre la réactivité des asphaltènes, une méthodologie innovante est proposée et validée. Une opération d'ultrafiltration par séparation membranaire tangentielle est mise au point afin de diminuer en amont la polydispersité des agrégats asphalténiques. Parallèlement, une méthode de reconstitution de charges permettant de disperser les asphaltènes dans leur matrice malténique d'origine est également développée. Les tests catalytiques effectués démontrent que cette méthode de reconstitution de charge (précipitation puis re-dispersion des asphaltènes) permet de conserver la réactivité naturelle des asphaltènes dans des conditions d'hydrotraitement. Dans de futurs travaux, l'utilisation de cette méthodologie permettra d'étudier l'influence de la taille des agrégats asphalténiques sur la réactivité en hydrotraitement, en reconstituant des charges avec des agrégats de taille variables et contrôlés.

Abstract — Asphaltene Cross-flow Membrane Ultrafiltration on a Preparative Scale and Feedstock Reconstitution Method — In order to understand asphaltene reactivity under hydrotreatment conditions, a new strategy is proposed. A cross-flow membrane ultrafiltration method is applied in order to control asphaltene aggregate size polydispersity. At the same time, a feedstock reconstitution method that allows asphaltene dispersion in maltenes is established. Catalytic tests are carried out, showing that the developed feedstock reconstitution method allows one to preserve asphaltenes' natural reactivity under hydrotreatment conditions. In further studies, the developed methodology will allow the study of the effect of asphaltene aggregate size on hydrotreatment activities by the reconstitution of feedstocks containing controlled aggregate size.

INTRODUCTION

Worldwide trends indicate a decline in the availability of conventional crude oil, which is balanced by the increasing exploitation of heavy crude. This trend makes it crucial to have modern refineries adapted to the upgrading of distillation petroleum residues.

Petroleum residues contain high quantities of sulfur that can be eliminated by hydrotreatment (HDT) using fixed bed units (Leprince, 1998). From this process an ultra-low sulfur fuel can be obtained, as well as a product that can be further upgraded in a Residue Catalytic Cracker (RCC).

Petroleum residues also contain asphaltenes and metals such as Ni and V, which are poisons to the HDS catalysts. For this reason these processes are divided into two sections (Kressmann *et al.*, 1998). The first section is dedicated to the elimination of asphaltenes and metals from the feedstock (HDM section), sulfur is then deeply removed in the HDS section.

This process configuration makes HDS catalysts' lifetime highly dependent on HDM catalyst performance. In order to maximize HDS performances more effort needs to be made in the development of new HDM catalysts as well as in the understanding of HDM reactions and asphaltene conversion.

By definition asphaltene is the most polar fraction of crude oil and it precipitates in the presence of a high excess of a normal alkane (nC_5 , nC_6 or nC_7), although it is soluble in toluene (Speight, 1999). The remaining fraction is called maltenes. Within an asphaltene fraction a large polydispersity of molecules exists, in terms of size, chemical composition and structure (Szewczyk *et al.*, 1996; Mullins *et al.*, 2000; Sheu, 2002). As a consequence, model molecules cannot be representative of all the chemical variety existing in an asphaltene sample. Besides, depending on parameters such as temperature, pressure, concentration and feedstock composition, these molecules can associate themselves and form aggregates with higher molecular weights (Merdrignac *et al.*, 2007) and large size polydispersity (Fenistein *et al.*, 2007; Barré *et al.*, 2008). This association-dissociation phenomenon is hard to explain and still not well understood, especially under hydroprocessing conditions (high temperature, high pressure, varying feedstock composition due to conversion) where asphaltene aggregate size should be decisive to conversion.

Some works suggest that asphaltene conversion requires a first dissociation step where the High-Molecular-weight (HMw) asphaltenes will first dissociate into Lower-Molecular-weight species (LMw). Dissociation should then be followed by cracking of adjacent aromatic structures, removal of naphthenic parts and/or dealkylation of aliphatic chains (Merdrignac *et al.*, 2006; Gauthier *et al.*, 2008). In this process, lighter fractions are formed where intermediate radical species are supposed to be stabilized by hydrogenation.

The first dissociation step is especially enhanced under hydroconversion conditions due its severe operating conditions. The same conversion mechanism is supposed to occur under hydrotreatment conditions, but to a lesser extent due to the lower severity. From this, we could imagine that HMw asphaltene aggregate species exist even when submitted to HDT conditions and will present different reactivities from LMw asphaltenes.

This aspect is explored in the development of simulating residue hydroprocessing models such as THERMIDOR (Toulhoat *et al.*, 2005). However, to discriminate the behavior and reactivity of asphaltenes with different sizes under hydrotreatment conditions remains a challenge of major importance.

Moreover, detailed characterization of the asphaltenes is hard to achieve and may be a real limitation for a better comprehension of the fundamental mechanisms in which they are involved during HDT processes.

Within this framework, in order to better understand asphaltenes conversion and to overcome difficulties such as:

- sample complexity (polydispersed species);
- association-dissociation phenomenon;
- model molecules not representative of AsC_7 variety;
- analytical limitations;
- defining a suitable lab-scale catalytic test representative of the HDT process.

We propose the following strategy schematized in Figure 1.

Because model molecules cannot be representative of all asphaltene varieties, this strategy consists in working with real asphaltenes whose matrix is first simplified by fractionating them into reduced polydispersed species. Only then is each fraction characterized using the available analytical techniques. Thus, the average detailed characterization results obtained for each fraction are more meaningful.

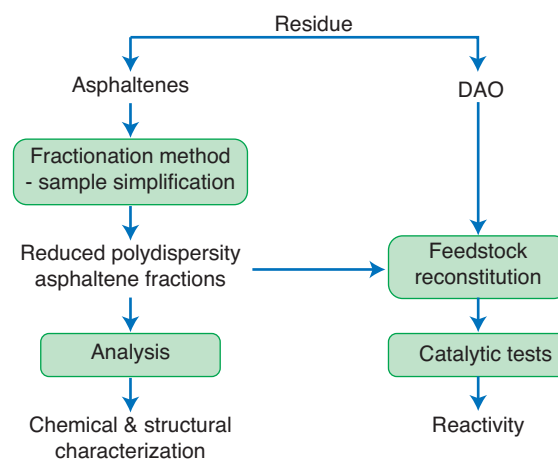


Figure 1

Proposed strategy to understand asphaltene conversion.

Also, in the scope of this work the reduced polydispersed asphaltene fractions will be used to reconstitute feedstocks using the original maltenes (deasphalted oil - DAO). Following this strategy, feedstocks containing selected types of asphaltenes (in terms of aggregate size) in the desired proportions can be obtained. These can be taken into account as reconstituted model feedstocks containing real asphaltenes dispersed in their original maltenes.

These reconstituted feedstocks can then be evaluated in a lab-scale catalytic test that simulates hydrotreatment conditions. Reactivity differences will be a direct consequence of asphaltenes' nature, present in each reconstituted feedstock.

In a recent work, ultrafiltration was found to be an adequate technique to separate asphaltene aggregates with different sizes at high selectivity in a lab-scale batch membrane filtration unit (Marques *et al.*, 2008). Using nanofiltration techniques, other relevant recent studies searched to relate the impact of asphaltene aggregate size on coke deposition on hydroprocessing catalysts (Zhao and Shaw, 2007, 2008).

The aim of this work will be to present the results of a home-made continuum cross-flow membrane filtration unit applied to fractionating asphaltene aggregates with different sizes without the limitations detected in batch-operated filtration units. Also, a feedstock reconstitution method will be proposed and validated.

Catalytic tests carried out to understand asphaltene reactivity will make the subject of further studies.

1 EXPERIMENTAL

1.1 Initial Asphaltene Sample Preparation

The asphaltenes used in this study were *n*-heptane (nC_7) insoluble fractions of a Safaniya vacuum residue. The main properties of the Safaniya VR are summarized in Table 6.

In order to obtain a large amount of asphaltenes (kilogram range), deasphalting was processed in a pilot unit at a temperature range from 210 to 230°C using a volume ratio of *n*-heptane to vacuum residue equal to 8. The mixture was stirred for one hour in a special home-made reactor unit and then settled for two hours in order to recover flocculated asphalts. We must specify that these asphalts are a mixture of the nC_7 asphaltenes and residual maltenes. The asphalt settles inside the reactor and the deasphalted VR phase was recovered on top of the reactor at a temperature close to 210°C. Flocculated asphalts were further recovered by addition of a large amount of toluene at 90°C inside the reactor. In order to remove the toluene, the asphalt phase was dried at 100°C under a N_2 atmosphere. After toluene evaporation, the obtained asphalts still contain 28 wt% of maltenes. Maltenes were then removed in a lab-scale deasphalting unit using a *n*-heptane to asphalt fraction ratio equal to 8. This mixture is

stirred for one hour at boiling temperature and then settled in order to recover flocculated asphaltenes. After cooling down, the suspension was then filtered using a Durapore PVDF 0.45 μm filter. Precipitated asphaltenes were then dried in an oven at 60°C. Also, *n*-heptane from the residual maltene fraction was eliminated by vacuum evaporation. These maltenes were then remixed with the deasphalted VR.

1.2 Asphaltene Fractionation by Cross-flow Membrane Filtration

The experimental setup consists of a filtration cell housing flat membrane sheets. It allows a continuous operation and displays 280 cm^2 of active filtration surface. This device contains a 140 mL hold-up volume and recycles the retentate stream at 500 L/h.

Asphaltenes were filtrated using a polyethersulfone porous membrane with a 20 kDa molecular weight cut-off (MWCO) (UP020 membrane produced by NADIR and provided by Alting, Hoerd France). Membranes were calibrated by the supplier using polysaccharide and polyethylene glycol. Membrane conditioning was first performed using toluene, at 10 bar and 25°C. In a previous work (Marques *et al.*, 2008), toluene was found to be adequate for asphaltene dispersion and to be compatible with the membrane material. NormapurTM 99.5%, VWR toluene was used after distillation and water elimination using a VWR Prolabo 3 Å molecular sieve.

The asphaltene sample was then dissolved in toluene (2 wt%) and filtrated until asphaltenes were no longer found in the permeate stream. During operation the asphaltene concentration in the retentate is maintained between 1 and 2 wt% by controlling the toluene make-up. After 40 h, membranes were replaced in order to verify if fouling occurs.

The filtrate and retentate fractions were recovered and toluene was then removed by vacuum evaporation.

Asphaltenes were characterized as described in Section 1.5.

1.3 Catalyst Sulfidation and Catalytic Test

Fresh commercial HDM catalysts were sulfided *ex-situ*, at 350°C (5°C/min heating ramp), for 2 h, under a 2 L/h/ $g_{catalyst}$ (15% H_2S /85% H_2) flow.

The catalytic test was conducted in an isothermal 300 mL batch reactor operated in fixed bed conditions summarized in Table 1.

A simplified scheme of the batch reactor is presented in Figure 2.

The reactor is first purged with hydrogen to eliminate air and is tested for leaks using high-pressure hydrogen. Leak testing is performed for 12 h at 100 bar. The reactor is then

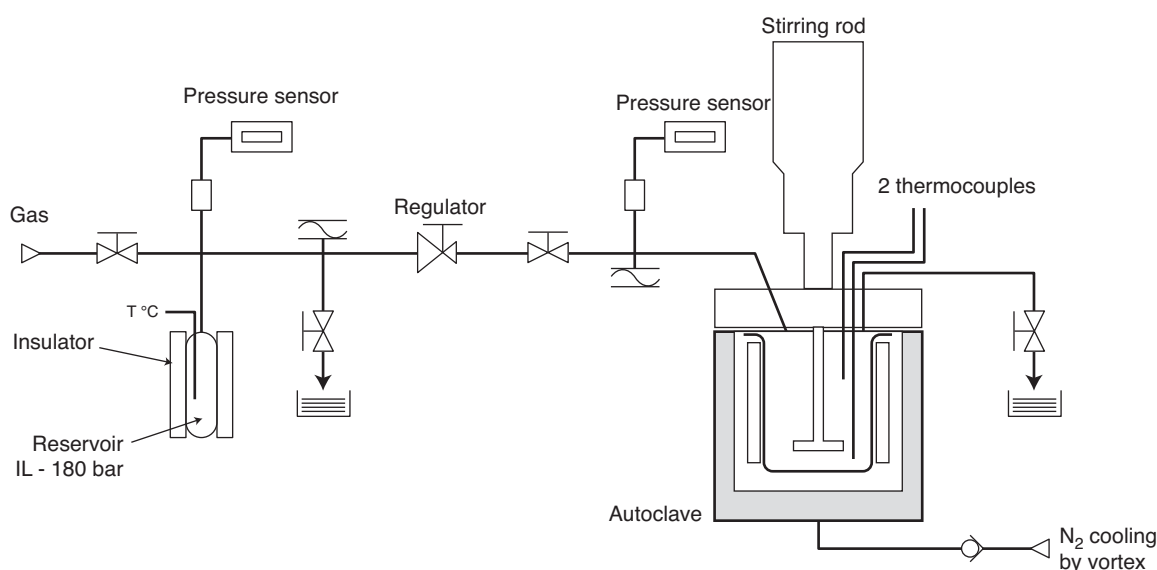


Figure 2

Batch reactor experimental setup.

depressurized to 40 bar and heated up from room temperature to the test temperature (370°C) at 20°C/min in a reproducible way. The pressure is generated by the temperature increase and is maintained constant during the test by a hydrogen make-up. The hydrogen consumption is determined by following the pressure drop in the make-up hydrogen tank. Reaction time is counted 30 min after the heating and pressure stabilization phase. The catalytic test is performed for 2 h (reaction time equivalent to 0.33 h contact time for 60/10 feed/catalyst volume ratio) at constant temperature (370°C) and pressure (95 bar).

TABLE 1
Operating conditions

P (bar)	95
T (°C)	370
$V_{catalyst}$ (cm ³)	10
$V_{feedstock}$ (cm ³)	60
$t_{reaction}$ (h)	2
$t_{contact}$ (h)	0.33
Stirring (rpm)	800

Contact time is defined as follows (Eq. 1):

$$t_{contact} = t_{reaction} \times \frac{V_{catalyst}}{V_{feedstock}} \quad (1)$$

At the end of the test the reactor is cooled down using an air vortex cooling system, which allows one to decrease temperature from 370°C to 150°C in 5 minutes. The final

product is recovered at 100°C. Feed and products are characterized by the techniques summarized in Table 2.

TABLE 2
Feedstock and product characterization techniques

Measure	Analytical methods	Standard
Ni, V, S	X-ray fluorescence	IFP standard
N	DUMAS	ASTM D5291
AsC ₇	Deasphalting	NFT60-115/82
CCR	Conradson Carbon	NF EN ISO 10370/95
Conversion	Simulated distillation	IFP standard

Nickel, vanadium, sulfur, asphaltenes, nitrogen and Conradson carbon hydrotreatment conversions (HDNi, HDV, HDS, HDAsC₇, HDN and HDCCR, respectively) are defined as follows:

$$HDX = \frac{m_{feed} [X]_{feed} - m_{product} [X]_{product}}{m_{feed} [X]_{feed}} \times 100 \quad (2)$$

where $[X]$ stands for Ni, V, S, N, AsC₇ and CCR content in the feedstock or in the product and m is the mass of product and feed.

Conversions (X_{T^+}) were obtained through Equation (3).

$$X_{T^+} (\%) = \frac{m_{feed} \times (x_{T^+})_{feed} - m_{product} \times (x_{T^+})_{product}}{m_{feed} \times (x_{T^+})_{feed}} \times 100 \quad (3)$$

where X_{T^+} is the conversion of fractions with boiling point superior to T temperature (T^+) into fractions with boiling point inferior to T temperature (T^-); x_{T^+} is the weight fraction of compounds with boiling points superior to T temperature (T^+). x_{T^+} fractions were obtained by simulated distillation analyses.

At the end, spent catalysts are collected and extracted with toluene in a Soxhlet extractor for 7 h, at atmospheric pressure ($T_{\text{Soxhlet}} = 250^\circ\text{C}$) and dried under vacuum at 140°C , for 4 h.

1.4 Feedstock and Product Characterization

Feeds and products are characterized by the techniques summarized in Table 2.

The main properties of the Safaniya Vacuum Residue (VR) used as reference feedstock are summarized in Table 6.

1.5 Characterization of Asphaltene Fractions

The different asphaltene fractions were characterized by Size-Exclusion Chromatography (SEC) for molecular weight distributions, Small-Angle X-ray Scattering (SAXS) for average radius of gyration and molecular weight measurement, elemental analysis for C, H, N, S, Ni and V content determinations, and nuclear magnetic resonance (^{13}C -NMR) for structural characterization.

It is well known that SEC and SAXS results may differ because:

- The aggregation state of asphaltenes is not the same in both experiments:
 - a different solvent is used (toluene in SAXS and THF in SEC);
 - SAXS measurements are carried out on rather highly concentrated asphaltene suspensions, a few percent of asphaltenes in toluene, instead of SEC experiments were the concentration of asphaltene entities flowing through the gel is probably very low (below a tenth of percent).
- SAXS measurement gives the weight average molecular weight (M_w – see Eq. 5), which is very dependent on the largest molecules. SEC data are given in equivalent polystyrene (eq. PS.), and SEC fractionation is mainly dependent on the hydrodynamic volume of the molecule. So, in these experiments the hydrodynamic volume of one asphaltene molecule is compared to the hydrodynamic volume of a polystyrene chain. There is evidence that the chemical structures of these entities are very different and thus different molecules can have similar hydrodynamic volume, but not identical molecular weight. To gain insight into this field it would be necessary to perform a universal calibration (Allcock *et al.*, 2003), taking into account not the average molecular weight of asphaltenes and polystyrene standards but the product of the intrinsic viscosity and the molecular weight ($[\eta]M$). This needs the

determination of the intrinsic viscosity of asphaltene molecules as a function of their molecular weight. Work is still in progress in this domain;

- Special adsorption effects exist on the SEC column, due to interaction between asphaltenes and the cross-linked polystyrene support.

1.5.1 Size-Exclusion Chromatography (SEC)

SEC was performed on a Waters Alliance 2695 system, using a refractive index detector described elsewhere (Merdrignac *et al.*, 2004). The system was controlled using an Empower chromatography manager. Calibration was performed using 10 monodisperse polystyrene standards with masses in the range of 162-120000 g/mol (Polymer Laboratories). Samples were injected at a concentration of 5 g/L in tetrahydrofuran (THF) with a volume of 50 μL . The temperature was adjusted to 40°C and the flow rate was fixed to 0.7 mL/min. Three columns that were packed with polystyrene-divinylbenzene supports (PS-DVB, Polymer Laboratories) were chosen; the corresponding porosities are 10, 100 and 1000 nanometers. The column characteristics are the following: packing particle size, $dp = 5 \mu\text{m}$; column length, $L = 300 \text{ mm}$; and internal diameter, 8 mm. The SEC data enable one describe the weight distributions according to weight averages, calculated as follows:

$$M_n = \frac{\sum N_i M_i}{\sum N_i}, \text{ number-average molar mass} \quad (4)$$

$$M_w = \frac{\sum N_i M_i^2}{\sum N_i M_i}, \text{ weight-average molecular mass} \quad (5)$$

where N_i represents the number of molecules with a molecular weight of M_i . Basically, M_n is more sensitive to low molecular weights, instead of higher orders of the distributions, M_w , which is sensitive to higher molecular weights.

1.5.2 Small-Angle X-ray Scattering (SAXS)

SAXS measurements were performed with a Huxley-Holmes type camera. The X-ray beam was provided by a copper (1.54 \AA) rotating anode (Rigaku); The X-ray beam was focused by a parabolic mirror with graded multilayer coating (Xenocs). A one-dimensional position-sensitive proportional counter (Elphyse) was used for X-ray spectrum recording. This detector has a resolution of 150 μm (full width at half maximum); the X-ray generator was operated at 1 kW (40 kV \times 25 mA). The range of wave vectors (q) accessible was between 0.01 and 0.22 \AA^{-1} . The asphaltene powders were diluted at 2-3 wt% in Rectapur grade toluene (VWR International), used as received without further purification, and allowed to stand overnight to avoid any kinetic effects.

The asphaltene solutions were introduced into a 2 mm diameter sealed glass capillary maintained in a temperature-controlled sample holder. After normalization in respect to thickness, transmission and measuring time, the solvent signal was subtracted from the sample signal. Experimental data were converted into scattering cross-section $I(q)$ in absolute scale (cm^{-1}). All the present experiments were conducted at 25°C.

The scattering cross-section $I(q)$ is measured as a function of the wave-scattering vector q defined by:

$$q = \frac{4\pi \times \sin\theta}{\lambda} \quad (6)$$

with λ : the wavelength and 2θ : the scattering angle.

For a two-component system, such as a particle in a solvent (in our case, asphaltenes in toluene), a general expression of $I(q)$ can be derived:

$$I(q) = \phi(1 - \phi)\Delta\rho^2 F(q)S(q) \quad (7)$$

with ϕ : particle volume fraction, $\Delta\rho^2$: contrast term (determined from specific gravity and chemical composition of solvent and particles), $F(q)$: the form factor ($F(0) = v$, volume of the scattering particle), which is a function of the shape, size and polydispersity of particles, and $S(q)$: the structure factor which depends on the inter-particle interactions. For this study, the specific gravity of asphaltene was estimated from the H/C ratio *versus* density correlation established by Fenistein (Fenistein, 1998).

For dilute solutions of particles, the structure factor can be neglected ($S(q) = 1$) and it has been shown (Barré *et al.*, 2008) that this approximation is valid up to a few percent of asphaltene in toluene. In the Guinier region (for small q values, that is to say, on scales larger than the typical size of particles), we can determine the scattering cross-section at zero angle $I(0)$ and the radius of gyration of the particles thanks to Zimm's approximation:

$$\frac{1}{I(q)} = \frac{1}{I(0)} \left(1 + \frac{q^2 R_g^2}{3} + \dots \right), \text{ for } qR_g \ll 1 \quad (8)$$

From Equation (7), $I(0)$ takes a simple form for dilute solutions from which the particle volume v can be extracted:

$$\frac{I(0)}{\phi\Delta\rho^2} = v \quad (9)$$

The "molar mass" M can be derived by using the usual expression:

$$M = dN_a v \quad (10)$$

with d the specific gravity of the solute and N_a the Avogadro number.

Combining (8), (9) and (10) one gets

$$\frac{I_e \Delta\rho^2}{d^2 N_a} \frac{c}{I(0)} = K \frac{c}{I(0)} = \frac{1}{M_w} \quad (11)$$

The molar mass and the radius of gyration of particles were determined from a least-square linear fit of $1/I(q)$ as a function of q^2 (Zimm plot).

1.5.3 ^{13}C Nuclear Magnetic Resonance (^{13}C -NMR)

NMR experiments were performed with an Advanced 300 MHz Bruker spectrometer, using a 10 mm BBO $^1\text{H}/\text{X}/\text{D}$ NMR probe. The chemical shifts were referenced using deuterated chloroform (CDCl_3) as a solvent. Samples were prepared by mixing 100 mg of asphaltenes in 3 mL of CDCl_3 to obtain a homogeneous solution. ^{13}C -NMR direct acquisition spectra were realized with a 60° flip angle at a radio frequency pulse of 20 kHz, which provided the quantity of saturated and unsaturated carbon atoms. In addition, two ^{13}C -NMR experiments, based on the scalar coupling between proton and carbons, were realized in order to obtain data about paraffinic, naphthenic and aromatic carbon species. The spin-echo experiment allowed the aromatic and aliphatic carbon species to be quantified separately, and the Attached Proton Test (APT) series was applied to identify and quantify the proportion of carbon atoms, as a function of the number of protons in their neighborhood.

2 RESULTS AND DISCUSSION

2.1 Fractionation Yields

Figure 3 represents the filtrate asphaltene flux as a function of filtration time. Asphaltene filtrate flux is defined as follows:

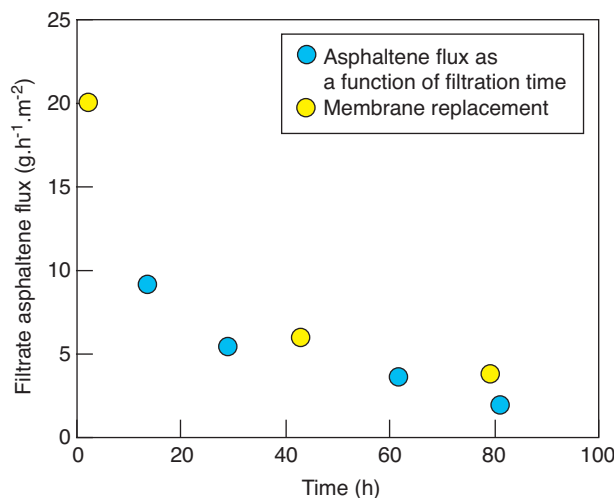


Figure 3

Filtrate Asphaltene Flux

$$= \frac{\text{filtrated asphaltene mass}}{\text{filtration time} \times \text{membrane surface}} \left(\frac{\text{g}}{\text{h.m}^2} \right) \quad (12)$$

It shows that the same flux is obtained if the membrane is replaced by a new one, meaning that the progressive flux reduction is not caused by membrane fouling. Asphaltenes smaller than membrane cut-off are progressively removed from the retentate fraction, explaining why their filtrating flux decreases. After 80 h, filtrated asphaltene flux is almost zero, meaning that a complete fractionation was accomplished. This shows that under these operating conditions the HMwAsC₇ in the retentate fraction maintain their aggregation state (*i.e.* they do not dissociate into LMwAsC₇ in order to re-establish their initial polydispersity). Otherwise, all the initial asphaltenes would have been recovered in the filtrate fraction.

This is also supported by the SEC results presented in Figure 5, showing that even under SEC conditions (dissolved in THF and analyzed at 40°C) the retentate asphaltenes concentrate mainly the high-molecular-weight species and the filtrate asphaltenes contain the lower-molecular-weight species.

The continuous cross-flow filtration device is equipped with a toluene make-up which allowed the complete segregation of asphaltenes. This could not be accomplished with batch devices used in previous work (Marques *et al.*, 2008).

It was found that HMwAsC₇ species represent 78 wt% of initial asphaltenes and only 22 wt% correspond to LMwAsC₇ species (Fig. 4). In this, operation losses represented 3 wt% of total asphaltenes.

2.2 Asphaltene Fraction Characterization

2.2.1 Colloidal Characterization

SEC chromatograms of collected asphaltene fractions are presented in Figure 5. These results show that asphaltenes from the filtrate fraction present lower average molecular masses (in eq. PS.) when compared with asphaltenes from the retentate fraction. Also, the polydispersity index (defined by $PDI = M_w/M_n$) indicates that the variety of species existing in the filtrate fractions, and to some extent in the retentate fraction, is lower than the variety of species existing in the initial fraction. Size polydispersity has been successfully reduced.

These relative mass profiles determined by SEC are complemented by the absolute average masses estimated by SAXS. These results are presented in Table 3, from which we can confirm the existence of substantial differences between retained and filtrated average aggregate size. SAXS estimates an average gyration radius of 158 Å for HMwAsC₇

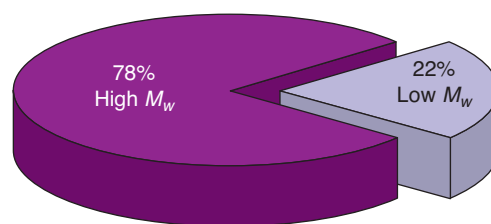
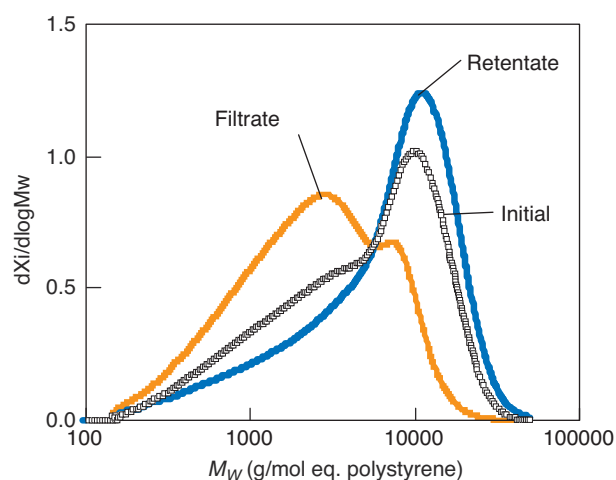


Figure 4

Distribution of asphaltene species (wt%); High M_w – Asphaltenes in the retentate fraction, Low M_w – Asphaltenes in the filtrate fraction.



	M_n (g/mol) eq. PS.	M_w (g/mol) eq. PS.	PDI
Initial	2039	7027	3.45
Retentate HMwAsC ₇	2684	9038	3.37
Filtrate LMwAsC ₇	1339	3637	2.72

Figure 5

SEC results of initial, retentate and filtrate asphaltenes.

aggregates (equivalent to $5.6 \times 10^5 \text{ g}\cdot\text{mol}^{-1}$) and 33 Å for LMwAsC₇ aggregates (equivalent to $0.23 \times 10^5 \text{ g}\cdot\text{mol}^{-1}$). These mass results are in good agreement with the membrane cut-off certified by the membrane supplier (calibration tests performed using polysaccharide and polyethylene glycol molecules).

Moreover, great differences are found between mass values obtained by SAXS and those obtained by SEC. Several interpretations for these discrepancies were presented and discussed previously in Section 1.5. The asphaltenes are not measured in the same aggregation state (different solvent and different conditions). Also, SAXS measurement gives the

average molecular weight, which is very dependent on the largest molecules. SEC data are given in equivalent polystyrene (eq. PS.) and are mainly dependent on the hydrodynamic volume of the molecule.

TABLE 3

SAXS characterization results for initial, retained and filtrate asphaltene fractions obtained by cross-flow ultrafiltration

	R_g (Å)	M_w (g.mol ⁻¹)*
Initial	116	3.3×10^5
Retentate HMwAsC ₇	158	5.6×10^5
Filtrate LMwAsC ₇	33	0.23×10^5

* Estimated by Fenstein correlation (Fenstein, 1998).

2.2.2 Chemical Characterization

Table 4 presents the average elemental composition (CHNOS). In order to confirm elemental analysis results, a mass balance for each element was made and a deviation parameter was calculated by Equation (13). This parameter expressed the deviation between element X content existing in the IAsC₇ fraction and the content present in both HMwAsC₇ and LMwAsC₇.

See Equation (13)

where $[X]_{\text{IAsC}_7}$, $[X]_{\text{LMwAsC}_7}$ and $[X]_{\text{HMwAsC}_7}$ represent the element X content in initial, low and high-molecular-weight asphaltene fractions, respectively; η_{LMwAsC_7} and η_{HMwAsC_7} stand for the obtained fractionation yields (Fig. 4).

Mass balance deviation results (Dev) are presented in Table 4. This shows that elemental composition is very

similar for both fractions (LMwAsC₇ and HMwAsC₇). Nevertheless, LMwAsC₇ and HMwAsC₇ oxygen content is overestimated at 38%. This could be due to analysis uncertainty or oxidation.

LMwAsC₇ present significantly lower metal content (Ni and V) and they preferentially concentrate vanadium in relation to nickel (lower Ni/V) when compared with HMwAsC₇ (higher Ni/V). This indicates that metals (Ni and V) are differently distributed within asphaltene polydispersity. It can be seen that although LMwAsC₇ represent 22 wt% of initial asphaltene, this fraction contains only 13% of the total Ni existing in the initial fraction.

All other elements seem to be equally distributed between the two fractions.

These aspects can be useful for the understanding of differences between HDV and HDNi conversions in the hydrotreating process and for the development of new hydrodemetallization catalysts.

Asphaltene chemical composition does not seem to explain their aggregation state. The aggregation behavior could mainly be related to structural properties which were evaluated by ¹³C NMR. However, Table 5 shows that no major differences are found within absolute average structure parameters of each fraction.

Within the aromatic and aliphatic relative results, minor trends can be pointed out when comparing HMwAsC₇ with LMwAsC₇:

- it seems that the existing aromatic structures are more condensed and also more substituted by aliphatic chains or naphthene structures in HMwAsC₇;

$$\text{Dev (\%)} = \frac{(\eta_{\text{LMwAsC}_7} \times [X]_{\text{LMwAsC}_7} + \eta_{\text{HMwAsC}_7} \times [X]_{\text{HMwAsC}_7}) \times m_{\text{IAsC}_7} - [X]_{\text{IAsC}_7} \times m_{\text{IAsC}_7}}{[X]_{\text{IAsC}_7} \times m_{\text{IAsC}_7}} \times 100 \quad (13)$$

TABLE 4

Elemental analysis results - initial asphaltene, HMwAsC₇ and LMwAsC₇ fractions obtained by cross-flow ultrafiltration (20 kDa, 10 bar, 25°C)

	Initial	HMwAsC ₇	LMwAsC ₇	Dev (%)
Carbon (wt%)	82.3 ± 0.4	81.9 ± 0.4	81.0 ± 0.4	-1%
Hydrogen (wt%)	7.5 ± 0.1	7.4 ± 0.1	7.3 ± 0.1	-2%
Nitrogen (wt%)	0.9 ± 0.2	0.9 ± 0.2	0.9 ± 0.2	2%
Oxygen (wt%)	1.2 ± 0.3	1.5 ± 0.3	2.2 ± 0.3	38%
Sulfur (wt%)	7.9 ± 0.2	7.6 ± 0.2	7.7 ± 0.2	-4%
H/C*	1.099	1.086	1.088	
N/C*	0.009	0.010	0.009	
O/C*	0.011	0.013	0.020	
S/C*	0.036	0.035	0.036	
Ni (ppm)	204 ± 7	223 ± 7	116 ± 4	-2%
V (ppm)	593 ± 31	605 ± 32	506 ± 26	-2%
Ni/V*	0.30	0.32	0.20	

*Atomic ratio.

TABLE 5

¹³C-NMR analysis results - initial asphaltenes, HMwAsC₇ and LMwAsC₇ fractions obtained by cross-flow ultrafiltration (20 kDa, 10 bar, 25°C)

	Initial AsC ₇	HMwAsC ₇	LMwAsC ₇	Initial AsC ₇	HMwAsC ₇	LMwAsC ₇
<i>C_{aromatic}</i> (wt%)	52 ± 2	50 ± 2	55 ± 2	<i>Relative to C_{aromatic}</i>		
<i>C_{aro}</i> quat condensed (wt%)	21 ± 2	20 ± 2	20 ± 2	41	40	36
<i>C_{aro}</i> quat. substituted (wt%)	21 ± 2	20 ± 2	19 ± 2	41	40	35
<i>Caro</i> -H (wt%)	9 ± 3	10 ± 3	16 ± 3	18	21	29
<i>C_{aliphatic}</i> (wt%)	48 ± 2	50 ± 2	45 ± 2	<i>Relative to C_{aliphatic}</i>		
<i>C_{ali}</i> quaternary (wt%)	0 ± 2	0 ± 2	0 ± 2	0	0	0
<i>C_{ali}</i> -H (wt%)	5 ± 3	12 ± 3	6 ± 3	11	23	12
<i>C_{ali}</i> -H ₂ (wt%)	32 ± 3	26 ± 3	28 ± 3	66	51	63
<i>C_{ali}</i> -H ₃ (wt%)	11 ± 3	13 ± 3	11 ± 3	23	26	24

- also, the higher relative Cali-H means that higher ramifications should exist within HMwAs₇ aliphatic structures;
- lower CH₂ indicates on average a lower length of aliphatic chains in HMwAsC₇;
- an identical CH₃ content is found, meaning that CH ramifications do not end up in the CH₃ carbon type, indicating that the extra ramifications probably connect different aromatic structures.

Attention must be paid when taking into account these results because differences are not very pronounced and remain close to the level of uncertainty of the measurements.

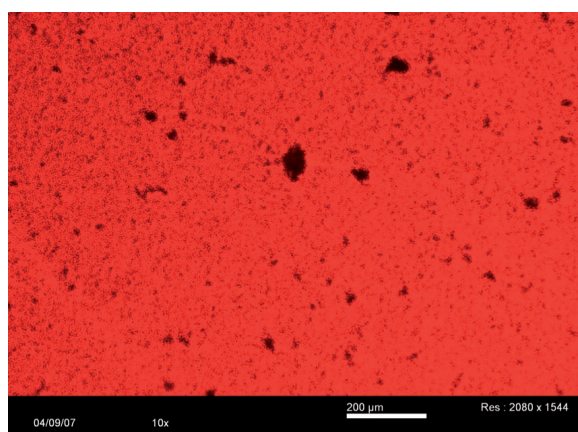
From elemental analysis and NMR results it is reasonable to assume that the chemical composition and structure of HMwAsC₇ and LMwAsC₇ are very similar. However, HMwAsC₇ concentrate more metals than LMwAsC₇, which indicates that structural and chemical differences can exist. These differences are not detected by NMR, probably because the characterization is limited to global average results.

2.3 Feedstock Reconstitution

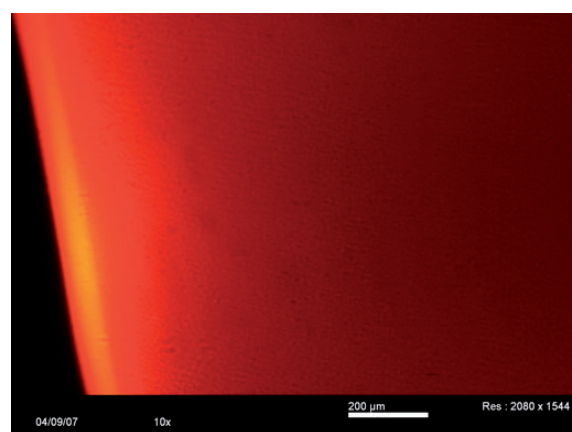
In order to understand asphaltene reactivity, feedstocks containing different types of asphaltenes need to be reconstituted. Within this framework a preliminary asphaltene dispersion study was performed using the IAsC₇ fraction and maltenes from the initial residue. This study consists of finding a method to re-disperse the extracted asphaltenes in the maltene fraction. Two protocols were used:

- asphaltene samples are crushed and mixed with maltenes by stirring at 80°C for 8 h;
- asphaltene samples are first dissolved in toluene (proportions 1:20). Then, this solution is mixed with maltenes and toluene is eliminated by vacuum distillation.

The reconstitution method was chosen based on optical microscope observations and was validated by comparing catalytic hydrotreating conversions from tests performed in the same conditions using the original residue and the reconstituted one.



a) Asphaltenes mixed directly with their original maltenes.



b) Asphaltenes first dissolved in toluene, then mixed with maltenes and final toluene elimination by evaporation under vacuum.

Figure 6

Optical microscope observation of reconstituted feedstocks.

2.3.1 Optical Microscope Results

Figure 6 shows the optical microscope observations from reconstituted feedstock using the two methods. This shows that direct dispersion (method a.) is inadequate or that more time is required to obtain a complete dispersion. In contrast, it seems that asphaltenes are completely dispersed using method (b.) by means of toluene pre-dissolution.

2.3.2 Reconstitution Methodology Validation - Catalytic Tests

Using this reconstitution method (b.), the extraction and redispersion of asphaltenes, could somehow modify the nature of the residue. Studies suggest that asphaltene precipitation could change their aggregation state further than just separating components (Reynolds *et al.*, 1986). Looking forward to validating the previously presented reconstitution methodology and taking into account the high complexity of asphaltene samples, we propose a reactivity test approach. This consists of comparing the results of a catalytic test performed in the exact same operating conditions but using the original feedstock in one case and using the reconstituted feedstock in the other.

Both feedstocks' characterization are presented in Table 6. Hydrotreatment functions were followed and the results are summarized in Figure 7.

TABLE 6

Original and reconstituted feedstock characterization

Composition	Original* VR	Reconstituted VR
Ni (ppm)	42.4 ± 0.4	37.9 ± 0.4
V (ppm)	142.8 ± 0.8	124.3 ± 0.8
S (wt%)	4.948 ± 0.014	4.765 ± 0.014
N (wt%)	0.40 ± 0.03	0.35 ± 0.03
AsC ₇ (wt%)	11.7 ± 1.8	11.6 ± 1.8
CCR (wt%)	20.1 ± 1.3	20.8 ± 1.3
SARA fractions		
Saturates (wt%)	11 ± 1	9 ± 1
Aromatics (wt%)	40 ± 1	39 ± 1
Resins (wt%)	34 ± 1	35 ± 1
Asphaltenes C ₇ (wt%)	13 ± 1	13 ± 1
Simulated distillation (wt%)		
370°C	1%	3%
500°C	9%	10%
540°C	17%	18%
560°C	22%	24%
580°C	29%	30%

*The original feedstock consists of a Safaniya vacuum residue.

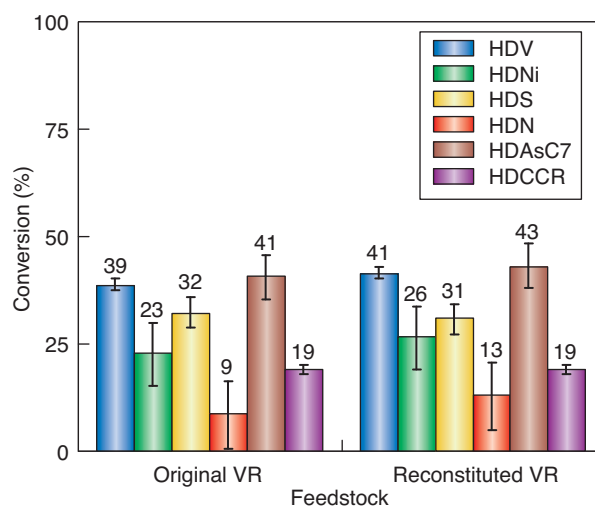


Figure 7

Comparison between original and reconstituted feedstock catalytic test performance of hydrotreatment functions.

These results show that the same conversions were obtained, meaning that the reconstitution methodology is valid. We can say that the asphaltene manipulation (extraction, redispersion in maltenes via dissolution in toluene followed by vacuum evaporation) did not affect the reconstituted sample in terms of catalytic performance.

Using this methodology, residues can be fractionated and reconstituted in a reproducible way.

CONCLUSION

Asphaltenes with different sizes were successfully obtained through a cross-flow membrane ultrafiltration process using a 20 kDa polyethersulfone membrane. It was seen that the LMwAsC₇ represent 22 wt% and HMwAsC₇ represent 78 wt% of the initial asphaltene aggregate sample, which is an important fact relevant to further interpretations.

- SEC and SAXS results confirmed that two distinct asphaltene fractions (in terms of aggregate size) are obtained:
SEC: M_w LMwAsC₇ ~ 3600 g.mol⁻¹ eq. PS; M_w HMwAsC₇ ~ 9000 g.mol⁻¹ eq. PS;
- SAXS: M_w LMwAsC₇ ~ 23000 g.mol⁻¹; M_w HMwAsC₇ ~ 560000 g.mol⁻¹.

In SAXS conditions, an average gyration radius of 158 Å is estimated for HMwAsC₇ and 33 Å for LMwAsC₇.

These results also confirm that the extraction of the LMwAsC₇ does not involve a further dissociation of the remaining HMwAsC₇ in LMwAsC₇ species during the membrane filtration.

The results obtained by ^{13}C -NMR have shown that the two asphaltene fractions present no significant differences in their average structures, despite the observed difference in average asphaltene aggregate size. Also, both fractions present a very similar chemical composition. Only metals are differently distributed between fractions. The HMwAsC₇ concentrate 30% more metals (Ni+V) than LMwAsC₇ and the Ni/V ratio is higher in HMwAsC₇ than in LMwAsC₇. These are crucial results to understand differences between HDM reactions.

To summarize, besides metal distribution these results indicate that the major difference between LMwAsC₇ and HMwAsC₇ is their size.

A reconstitution methodology was defined and proven to be adequate for reconstituting model feedstocks without influencing asphaltene natural reactivity.

In further studies, this methodology will be used to prepare reconstituted feedstocks with different asphaltene fractions (LMwAsC₇ and HMwAsC₇) to observe the effect of aggregate size on hydrotreating reactivity.

REFERENCES

- Allcock H.R., Lampe F.W., Mark J.E. (2003) *Contemporary Polymer Chemistry*, Pearson Education, Inc., New Jersey.
- Andersen S.I. (1994) Dissolution of solid Boscan asphaltenes in mixed solvents, *Fuel Sci. Technol. Int.* **12**, 1551-1557.
- Andersen S.I. (1997) Separation of asphaltenes by polarity using liquid-liquid extraction, *Petrol. Sci. Technol.* **15**, 185-198.
- Andersen S.I., Keul A., Stenby E. (1997a) Variation in composition of subfractions of petroleum asphaltenes, *Petrol. Sci. Technol.* **15**, 611-645.
- Andersen S.I., Keul A., Stenby E. (1997b) Variation in composition of subfractions of petroleum asphaltenes, *Petrol. Sci. Technol.* **15**, 611-645.
- Andersen S.I., Lira-Galeana C., Stenby E.H. (2001) On the mass balance of asphaltene precipitation, *Petrol. Sci. Technol.* **19**, 457-467.
- Barré L., Simon S., Palermo T. (2008) Solution properties of Asphaltenes, *Langmuir* **24**, 3709-3717
- Baltus R.E., Anderson J.L. (1983) Hindered diffusion of asphaltenes through microporous membranes, *Chem. Eng. Sci.* **38**, 1959-1969.
- Buenrostro-Gonzalez E., Groenzin H., Lira-Galeana C., Mullins O.C. (2001) The overriding chemical principles that define asphaltenes, *Energ. Fuel.* **15**, 972-978.
- Fenistein D. (1998) *PhD Thesis*, Université Paris VI, France.
- Fenistein D., Barré L. (2001) Experimental measurement of the mass distribution of petroleum asphaltene aggregates using ultracentrifugation and small-angle X-ray scattering, *Fuel* **80**, 283-287
- Gauthier T., Danial-Fortain P., Merdrignac I., Guibard I., Quoineaud A.A. (2008) Studies on the evolution of asphaltene structure during hydroconversion of petroleum residues, *Catal. Today* **130**, 429-438.
- Kressmann S., Morel F., Harle V., Kasztelan S. (1998) Recent developments in fixed-bed catalytic residue upgrading, *Catal. Today* **43**, 203-215.
- Leprince P. (1998) *Le raffinage du Pétrole : Procédés de transformation*, Editions Technip, Paris, Institut français du pétrole.
- Lira-Galeana C., Buenrostro-Gonzalez E., Garcia-Martinez J.A., Andersen S.I. (2002) Solubility/molecular structure relationships of asphaltenes in polar and nonpolar media, *Energ. Fuel.* **16**, 732-741.
- Marques J., Merdrignac I., Baudot A., Barre L., Guillaume D., Espinat D., Brunet S. (2008) Asphaltenes size polydispersity reduction by nano- and ultrafiltration separation methods - Comparison with the flocculation method, *Oil Gas Sci. Technol. - Rev. IFP* **63**, 139-149.
- Merdrignac I., Espinat D. (2007) Physicochemical characterization of petroleum fractions: The state of the art, *Oil Gas Sci. Technol. - Rev. IFP* **62**, 7-32.
- Merdrignac I., Quoineaud A.A., Gauthier T. (2006) Evolution of asphaltene structure during hydroconversion conditions, *Energ. Fuel.* **20**, 2028-2036.
- Merdrignac I., Truchy C., Robert E., Guibard I., Kressmann S.P. (2004) Size exclusion chromatography: Characterization of heavy petroleum residues. application to resid desulfurization process, *Petrol. Sci. Technol.* **22**, 1003-1022.
- Mullins O.C., Eser S., Mathews J., Yang M.G., Jones D., Groenzin H. (2003) Molecular size of asphaltene solubility fractions, *Energ. Fuel.* **17**, 498-503.
- Mullins O.C. Groenzin H. (2000) Molecular size and structure of asphaltenes from various sources, *Energ. Fuel.* **14**, 677-684.
- Murgich J. (2002) Intermolecular forces in aggregates of asphaltenes and resins, *Petrol. Sci. Technol.* **20**, 983-997.
- Neves G.B.M., de Sousa M.D., Travalloni-Louvisse A.M., Lucas E.F., Gonzalez G. (2001) Characterization of asphaltene particles by light scattering and electrophoresis, *Petrol. Sci. Technol.* **19**, 35-43.
- Portet M., Merdrignac I. (2006) *Fractionnement de macromolécules d'asphaltènes par solvant à l'échelle préparative*, 59156, IFP.
- Reynolds J.G., Biggs W.R. (1986) Effects of asphaltene precipitation and reprecipitation on the metal-containing compounds in heavy residua, *Fuel Sci. Technol. Int.* **4**, 779-798.
- Sane R.C., Tsotsis T.T. (1988) Hondo asphaltene diffusion in microporous track-etched membranes, *196th ACS Natl. Meet.*, 237-247.
- Sharma B.K., Stipanovic A., Tyagi O.S. (2000a) *Preprints ACS, 220th Nat. Meet., Div. Petr. Chem.* **45**, 643.
- Sharma B.K., Tyagi O.S., Aloopwan M.K.S., Bhagat S.D. (2000b) Spectroscopic characterization of solvent soluble fractions of petroleum vacuum residues, *Petrol. Sci. Technol.* **18**, 249-272.
- Sheu E.Y. (2002) Petroleum asphaltene - Properties, characterization and issues, *Energ. Fuel.* **16**, 74-82.
- Speight J.G. (1999) *The Chemistry and Technology of Petroleum*, 3rd ed., Dekker, New York.
- Szewczyk V., Behar F., Behar E., Scarsella M. (1996) Evidence of the physicochemical polydispersity of asphaltenes, *Revue de l'Institut Français du Pétrole* **51**, 575-590.
- Toulhoat H., Hudebine D., Raybaud P., Guillaume D., Kressmann S. (2005) THERMIDOR: A new model for combined simulation of operations and optimization of catalysts in residues hydroprocessing units, *Catal. Today* **109**, 135-153.
- Wattana P., Fogler H.S., Yen A., Garcia M.D., Carboognani L. (2005) Characterization of polarity-based asphaltene subfractions, *Energ. Fuel.* **19**, 101-110.

White L.S., Nitsch A.R. (2000) Solvent recovery from lube oil filtrates with a polyimide membrane, *J. Membrane Sci.* **179**, 267-274.

Zhao B., Shaw J.M. (2007) Composition and size distribution of coherent nanostructures in Athabasca bitumen and Maya crude oil, *Energ. Fuel.* **21**, 2795-2804.

Zhao B., Shaw J.M. (2008) Impact of asphaltene-rich aggregate size on coke deposition on a commercial hydroprocessing catalyst, *Energ. Fuel.* **22**, 1080-1092.

*Final manuscript received in July 2009
Published online in November 2009*

Copyright © 2009 Institut français du pétrole

Permission to make digital or hard copies of part or all of this work for personal or classroom use is granted without fee provided that copies are not made or distributed for profit or commercial advantage and that copies bear this notice and the full citation on the first page. Copyrights for components of this work owned by others than IFP must be honored. Abstracting with credit is permitted. To copy otherwise, to republish, to post on servers, or to redistribute to lists, requires prior specific permission and/or a fee: Request permission from Documentation, Institut français du pétrole, fax. +33 1 47 52 70 78, or revueogst@ifp.fr.